Article

J. Biol. Regul. Homeost. Agents. 2024; 38(7): 5583–5593
https://doi.org/10.23812/j.biol.regul.homeost.agents.20243807.449

^{18}F-FDG Positron Emission Tomography in Myocardial Viability Assessment: Oral Glucose and Intravenous Insulin Loading Protocol vs Fasting Status Protocol

Taoying Gu[1,2,3,4,*], Wujian Mao[1,2,3,4], Haojun Yu[1,2,3,4], Shuguang Chen[1,2,3,4], Xiangqing Wang[1,2,3,4], Hongcheng Shi[1,2,3,4,*]

[1]Department of Nuclear Medicine, Zhongshan Hospital, Fudan University, 200032 Shanghai, China
[2]Nuclear Medicine Institute of Fudan University, 200032 Shanghai, China
[3]Shanghai Institute of Medical Imaging, 200032 Shanghai, China
[4]Cancer Prevention and Treatment Center, Zhongshan Hospital, Fudan University, 200032 Shanghai, China
*Correspondence: 13564078731@163.com (Taoying Gu); shi.hongcheng@zs-hospital.sh.cn (Hongcheng Shi)
Submitted: 13 March 2024 Revised: 7 May 2024 Accepted: 10 May 2024 Published: 1 July 2024

Background: Determination of myocardial viability is vital for coronary revascularization in patients with ischemic cardiomyopathy (ICM). To select the appropriate strategies for ICM screening, the present study compared the image quality, viability extent, and dyssynchrony of ^{18}F-fluorodeoxyglucose (^{18}F-FDG) positron emission tomography (PET) myocardial viability imaging in patients with ICM using an oral glucose and intravenous insulin loading (G/I) protocol with a convenient fasting status (FAST).

Methods: ^{18}F-FDG PET metabolic imaging was conducted using the G/I and FAST protocols on different days and ^{99m}Tc-methoxyisobutylisonitrile (MIBI) perfusion imaging in all patients (N = 44). Fluorodeoxyglucose (FDG) image quality was assessed using a 5-point scoring system. The semiquantitative analysis included SUVmean of blood pool (SUVmeanBlood), SUVmax of the whole left ventricular muscle (SUVmaxMyo), and the SUVmeanBlood and SUVmaxMyo ratio (M/B). Furthermore, the quantitative analysis involved comparing the extent of mismatch on polar maps and evaluating left ventricle dyssynchrony between the two groups. The Cohen κ-test was used to investigate positive or negative on left anterior descending (LAD), left circumflex (LCX) or right coronary artery (RCA) between the groups.

Results: The imaging quality scores were 4.36 $\pm$ 0.94 and 3.55 $\pm$ 1.09 using the G/I and FAST protocols, respectively ($p < 0.001$). Significant differences were found in SUVmeanBlood, SUVmaxMyo, and M/B between the two groups ($p < 0.001$, 0.007, and $<$0.001, respectively). G/I and FAST protocols indicated good agreement for positive and negative findings in the LAD, LCX, and RCA (κ = 0.847, 0.858, and 0.74, respectively). Myocardial viability assessment exhibited equivalence between the two groups (all $p > 0.05$) within the imaging score ranging from 3 to 5. Furthermore, dyssynchrony assessment of left ventricle exhibited no significant difference between the two groups (all $p > 0.05$). For the G/I method, insulin consumption (95% confidence interval (CI) 0.03–0.27, $p = 0.014$) and SUVmaxMyo (95% CI 0.07–0.24, $p = 0.0005$) were identified as significant predictors for metabolic imaging score (coefficient of determination (R^2) = 0.6226). Similarly, for the FAST protocol, SUVmaxMyo (95% CI 0.09–0.29, $p = 0.0003$) was a significant predictor for metabolic imaging score (coefficient of determination (R^2) = 0.6787).

Conclusions: Our findings indicate that ^{18}F-FDG PET in assessing myocardial viability using the FAST protocol could be a time-efficient and safe option for clinical personalized practice.

Clinical Trial Registration: Chinese Clinical Trial Registry (ChiCTR2400083975).

Keywords: positron emission tomography; ^{18}F-fluorodeoxyglucose; hibernating; myocardial viability; glucose loading; fasting

Introduction

Determining ischemic myocardial viability is crucial for planning coronary revascularization in patients with ischemic cardiomyopathy (ICM) [1]. Various non-invasive imaging modalities are available to assess myocardial viability, primarily including dobutamine stress echocardiography (ECD), single-photon emission computed tomography (SPECT), late gadolinium enhancement cardiac magnetic resonance (LGE-CMR), and positron emission tomography (PET). Among these methods, metabolic imaging with ^{18}F-fluorodeoxyglucose (^{18}F-FDG) PET is the only Food and Drug Administration (FDA)-approved technique for assessing myocardial viability [2]. Furthermore, this is the most extensively studied and widely used technique, recognized as the "gold standard" technique for identifying viable myocardium [3,4].

Journal of
BIOLOGICAL REGULATORS
and Homeostatic Agents

Various protocols are used to promote ^{18}F-FDG uptake in the heart. The hyperinsulinemic-euglycemic clamp technique is regarded as the most effective method for enhancing ^{18}F-FDG uptake in the hibernating myocardium [5], especially for diabetic patients [6,7], but it is complicated and time-consuming. The oral glucose and intravenous insulin loading (G/I) protocol is the most common method in routine cardiac ^{18}F-FDG PET viability studies [2,6]. This technique is simpler than the clamp method but needs intravenous insulin administration, frequent blood glucose monitoring, and carries the risk of hypoglycemia. Several modified protocols are proposed to be practical and time-efficient [8], safer [9], or to improve quality [10,11] compared to the G/I method. Another ^{18}F-FDG PET metabolic study uses a fasting status protocol [12], referred to as fasting status (FAST), which is based on the preference of ischemic myocardium for glucose metabolism over fatty acids.

In contrast, normal myocardium primarily relies on fatty acid metabolism. However, there is a scarcity of literature comparing myocardial viability assessment between G/I and FAST protocols in a self-controlled manner. Therefore, this study aimed to evaluate the image quality, viability extent and dyssynchrony of ^{18}F-FDG PET metabolic imaging with G/I and convenient FAST protocols.

Materials and Methods

Study Subjects

This prospective study enrolled 44 consecutive ICM patients at Zhongshan Hospital, Fudan University, China, between August 2022 and April 2023. All the patients underwent self-controlled metabolic imaging using G/I and FAST methods. Diabetes mellitus (DM) was identified based on clinical history and fasting blood glucose (FBG) levels.

The inclusion criteria were as follows: (1) Individuals clinically diagnosed with ICM due to coronary artery disease (CAD) confirmed by coronary angiogram, past or present. (2) Those intended to undergo coronary artery bypass grafting (CABG). (3) The patients agreed to accomplish the entire study protocol. The exclusive criteria were as follows: The individuals with (1) concurrent malignant tumor, (2) concurrent cardiac sarcoidosis or infection, (3) pregnancy, (4) contraindications to DSPECT or PET/CT imaging, (5) inability to tolerate the whole study, and (6) normal ^{99m}Tc-methoxyisobutylisonitrile (MIBI) rest myocardial perfusion imaging (MPI).

This study was approved by the Medical Ethics Committee of Zhongshan Hospital, Fudan University (B2022-280R), and written informed consent was obtained from all the patients.

Study Protocol

Each study subject underwent ^{18}F-FDG PET/CT metabolic imaging using either G/I or FAST protocol on the first day in a randomized fashion, followed by the alternate method the next day. MPI was performed within one week to determine perfusion defects. Before imaging, diabetic patients were directed to avoid oral antidiabetic medications or insulin injections. FGB levels were assessed at the beginning of either the G/I or FAST method, with a fasting time of more than 6 hours.

Metabolic Preparation

The metabolic preparation protocol was performed by an experienced nurse and an observer in a dedicated preparation room.

Diabetes was defined as described previously [13–15], and either the G/I or FAST methods were used accordingly. For the G/I protocol, all study subjects followed a standard protocol involving oral glucose and intravenous insulin administration: (1) In diabetic patients, if FBG was $<$7.2 mmol/L, they orally received 12.5 g of glucose, otherwise, insulin was administered directly. (2) In non-diabetic patients, if FBG was $<$5.6 mmol/L, they orally received 50 g of glucose; if FBG $\geq$5.6 mmol/L, they orally received 25 g of glucose. The peak blood glucose (PBG) level was assessed 60 minutes later. Regular insulin was injected intravenously based on the observed PBG using a specific insulin dosage protocol (1, 2, 2, 3, 5, 6, 7, 8, 9 units of regular insulin for PBG ranges of 7.22–7.78, 7.78–8.89, 8.89–10, 10–11.11, 11.11–12.22, 12.22–13.33, 13.33–14.44, 14.44–15.56, $>$15.56, respectively). Those who received insulin directly used the above-mentioned insulin dosage protocol based on their FBG. Blood glucose (BG) levels were monitored at intervals between 20–30 minutes after insulin injection. Once the BG level reached a target range of 5.5–7.8 mmol/L (defined as pre-injected BG),^{18}F-FDG was administered intravenously. The PET imaging with fluorodeoxyglucose (FDG) was performed 2 hours after the FDG injection. BG was determined before the blood glucose before imaging (pre-image BG) to monitor the risk of hypoglycemia. The metabolic preparation period (MPP) was the interval between oral glucose loading and FDG injection. During the procedure, if a patient experienced symptomatic or asymptomatic hypoglycemia (serum glucose $<$70 mg/dL) after insulin administration, the protocol allowed oral intake of 10 g of glucose to maintain normal blood glucose levels. If such an event occurred within 30 minutes of the ^{18}F-FDG cardiac uptake period, the study was discontinued as it was expected that the ^{18}F-FDG PET images would be suboptimal quality.

For the FAST technique, all participants received intravenous injection of ^{18}F-FDG immediately after FBG was determined, followed by FDG PET imaging 2 hours after FDG injection. Pre-image BG levels were determined before imaging.

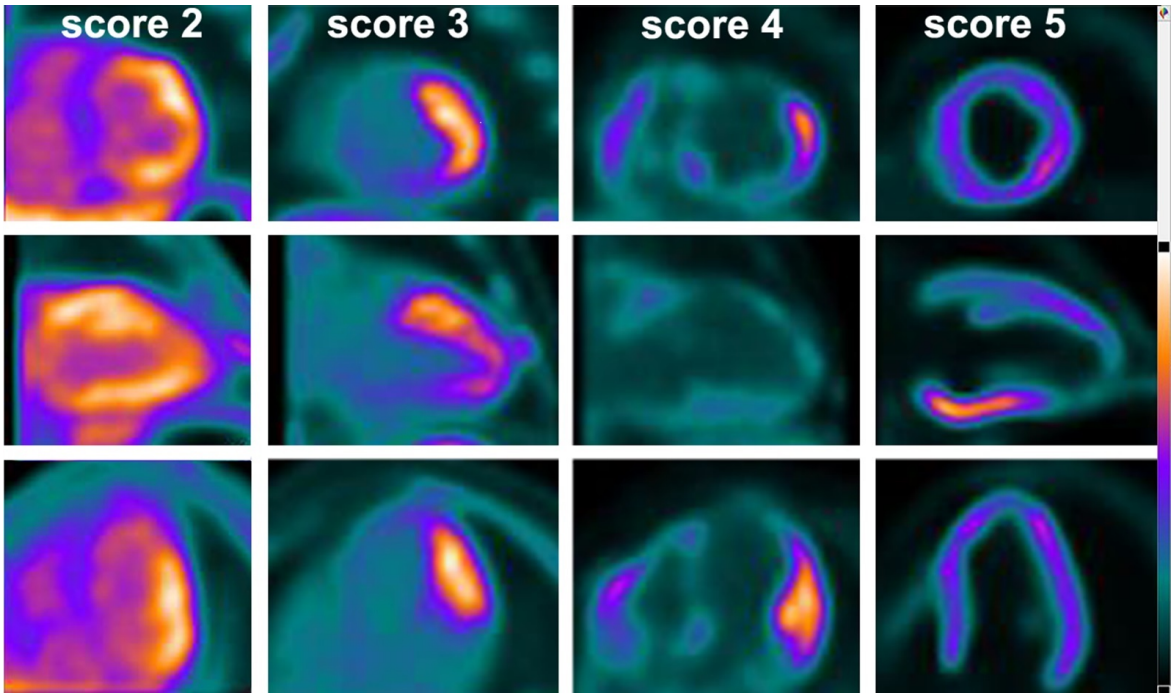

Fig. 1. Schematic diagram of the 5-point scoring system for left ventricle imaging quality. The top line, the short axis; the middle line, vertical long-axis; the bottom line, the horizontal long-axis. Score 1 (not shown in this study), non-diagnostic; score 2 (the first column), fair; score 3 (the second column), good; score 4 (the third column), very good; score 5 (the fourth column), excellent.

Metabolic Imaging Protocol

Metabolic images were acquired approximately 2 hours following ^{18}F-FDG administration (3.7 MBq/kg) using a total-body PET/CT scanner (uEXPLORER, United Imaging Healthcare (UIH), Shanghai, China) for all patients. Initially, a scout computed tomography (CT) was conducted (120 kV, 40 mA). After this, thoracic attenuation-corrected computed tomography (ACCT) was performed (120 kV, 9 mA) to ensure attenuation correction of PET data and precise anatomic structure recognition for accurate localization of ^{18}F-FDG uptake. All electrocardiogram (ECG) gating data (8 frames per RR circle) were reconstructed using a 3-dimensional ordered-subset expectation maximization protocol with 3 iterations and 20 subsets, incorporating time of flight data.

MPI Protocol

ECG gated rest MPI were obtained on D-SPECT cardiac scanner (Spectrum Dynamics, Caesarea, Israel) 90–120 minutes after injection, using a 64 × 64 × 38 acquisition matrix, a zoom factor of 1.0, and a total myocardial counts of 0.7–1.3 million counts. Image reconstruction was conducted using commercially available software Spectrum Dynamics Processing Station software (Version 2.7.1, Spectrum-Dynamics Medical, Caesarea, Israel) for reconstructing study operations. Subsequently, the transaxial views were imported for analysis with ^{18}F-FDG PET data using the Emory Cardiac Toolbox (ECTb, Version 4.0, Emory University, Atlanta, GA, USA).

Qualitative Analysis

By conducting the Spearman Correlation analysis, the qualitative assessment of ^{18}F-FDG PET images was performed by two independent and experienced nuclear medicine physicians. Any disagreements were resolved through a joint consensus reading.

A 5-point visual scoring system, similar to that utilized in previous study, was used [8]. Specifically, scores 2–5 (Fig. 1) showed homogenous or heterogenous ^{18}F-FDG signal, while score 1 indicated very low or absent ^{18}F-FDG-signal. Excellent image quality (score 5) was defined by absence of blood pool activity; very good image quality (score 4) exhibited mild blood pool activity; good image quality (score 3) showed moderate blood pool activity; fair image quality (score 2) indicated high blood pool activity; and non-diagnostic image quality (score 1) was linked to high blood pool activity.

The MPI and metabolic imaging data were analyzed utilizing ECTb (Version 4.0, Emory University, Atlanta, GA, USA). The perfusion-metabolism mismatch results were displayed using polar maps normalized to the maximum activity, exhibiting the percentage of territory in the three coronary arteries [total, left anterior descending (LAD), left circumflex (LCX), and right coronary artery (RCA)].

In this context, preservation of ^{18}F-FDG in a region with reduced perfusion is consistent with "viability" and indicates hibernation (perfusion-metabolism mismatch, with a threshold of 50% [16,17]). On the perfusion-metabolism

Journal of
BIOLOGICAL REGULATORS
and Homeostatic Agents

mismatch extent polar map, if the percentage of involvement in the total, LAD, LCX, or RCA is non-zero, it was considered positive for hibernating myocardium. In contrast, if the rate of involvement is zero, it was considered negative for hibernating myocardium.

Quantitative Analysis

In FDG PET images, the SUVmean of blood pool (SUVmeanBlood) was obtained by drawing a region of interest (ROI) of 0.5–1.0 cm^2 in the left ventricle (LV) near the mitral valve level [18]. The SUVmax of the whole left ventricular muscle (SUVmaxMyo) was assessed by placing a volum of interest (VOI) over the whole left ventricular muscle on the three-dimensional fused PET/CT images [10]. Furthermore, the SUVmeanBlood and SUVmaxMyo ratio (M/B) was calculated to assess the image quality quantitatively.

The extent of perfusion-metabolism mismatch percentage was quantitatively compared between the G/I and FAST groups for total, LAD, LCX, or RCA. Additionally, the two groups were compared regarding LV function and dyssynchrony.

Statistical Analysis

Statistical analysis was conducted using GraphPad Prism (v5, GraphPad, San Diego, CA, USA) and SPSS (v21, IBM Corp., Armonk, NY, USA) software. The normality of the data was determined using the Shapiro-Wilk test, the analysis of the mean and standard deviation (SD) of the data, and the quantile-quantile plot [19]. The Paired *T*-test was used to compare the normally distributed measurement data (expressed as mean ± SD) in both groups. Moreover, the non-normal measurement data (expressed as the median and the interquartile range) were compared using the Wilcoxon signed-rank test. The Cohen κ-test was used to investigate agreement (positive or negative) on LAD, LCX, or RCA of perfusion-metabolism extent mismatch polar map in both groups. Predictors for qualitative estimation (5-point score) were analyzed utilizing Spearman correlations. Furthermore, multiple linear regression was performed to quantify the relationship between image score and significant parameters. A *p*-value less than 0.05 was considered statistically significant.

Results

Baseline Characteristics of the Study Participants

The characteristics of all 44 ICM patients are summarized in Table 1. Among the 22 diabetic patients, 15 patients were treated with hypoglycemic agents, 4 with insulin, and 3 with a combination of both. Approximately half of all the patients presented with a history of previous myocardial infarction. Common risk factors such as hypertension, hyperlipidemia, and smoking were noted in more than 45% of the study participants. Left ventricular ejection fraction (LVEF) measured by ECD before imaging was less than 40% in 70.5% of patients. Severe coronary stenosis involving at least two vessels was observed in 88.6% of patients.

Table 1. Baseline characteristics of the study participants.

Parameters	Total number (mean ± SD)
Age (yrs)	59.66 ± 9.15
Male/female	40/4
Height (cm)	167.98 ± 6.98
Weight (kg)	67.89 ± 9.17
BMI	24.03 ± 2.67
ECD LVEF (%)	37.80 ± 9.61
Non-DM	22
DM	22
Prior PTCA/CABG	20
Prior MI	22
Hypertension	30
Smoking	25
Dyslipidemia	20

Note: The data were presented as mean ± standard deviation (SD) or number.

Abbreviations: Non-DM, non-diabetes mellitus; DM, diabetes mellitus; BMI, body mass index; ECD, echocardiography; LVEF, left ventricular ejection fraction; PTCA, percutaneous transluminal coronary angioplasty; CABG, coronary artery bypass grafting; MI, myocardial infarction.

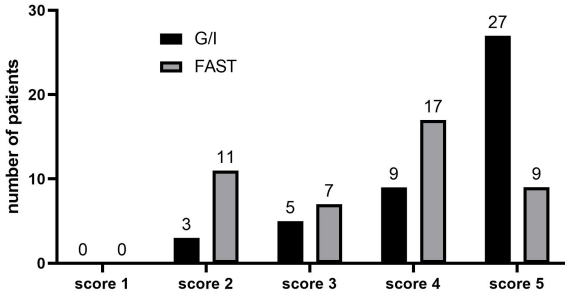

Fig. 2. Visual scale comparisons between the G/I and FAST groups. G/I, oral glucose and intravenous insulin loading; FAST, fasting status.

The clinical parameters and outcomes between the G/I and FAST groups are summarized in Table 2. The pre-image BG level in the G/I group (5.38 ± 0.88 mmol/L) was significantly lower than that in the FAST group (6.24 ± 1.50 mmol/L, $p < 0.001$). FBG and blood glucose before FDG injection (pre-inject BG) exhibited no statistically significant difference between the G/I and FAST groups ($p = 0.415$, $p = 0.768$, respectively). In the G/I group, more than 30 minutes after the FDG injection, one patient showed

Table 2. Comparison of various parameters between the G/I and FAST groups.

	G/I	FAST	*p*-value	*t* value
FBG (mmol/L)	6.48 ± 1.56	6.61 ± 1.72	0.415	–0.822
Pre-inject BG (mmol/L)	6.68 ± 0.69	6.61 ± 1.72	0.768	0.297
Pre-image BG (mmol/L)	5.38 ± 0.88	6.24 ± 1.50	<0.001*	–4.215
PBG	9.44 ± 1.79			
Insulin (U)	3 (2–5)			
MPP (min)	85.30 ± 32.35			
Side effect				
Symptomatic hypoglycemia	1	0		
Asymptomatic hypoglycemia	2	0		
Hunger	7	0		
Sweating	3	0		
Dizziness	1	0		
Fast heart rate	1	0		

Note: Normally distributed data were presented as mean ± SD, and non-normally distributed data were presented as the median and the interquartile range.

*p-value < 0.05 in comparison between G/I and FAST groups.

Abbreviations: G/I, oral glucose and intravenous insulin loading; FAST, fasting status; FBG, fasting blood glucose; pre-inject BG, blood glucose before FDG injection (reaching a target of 5.5–7.8 mmol/L in G/I group, equalling to FBG in FAST group); pre-image BG, blood glucose before imaging; PBG, peak blood glucose (assessed 60 minutes after oral glucose loading); MPP, metabolic preparation period, the period between oral glucose loading and FDG injection.

FBG was determined at the beginning of the G/I or FAST protocol with a fasting time of more than 6 hours.

Table 3. The positive and negative findings on total, LAD, LCX, or RCA of perfusion-metabolism mismatch extent polar map in the G/I and FAST groups.

Group	G/I							
FAST	Total		LAD		LCX		RCA	
	Positive	Negative	Positive	Negative	Positive	Negative	Positive	Negative
Positive	43	1	35	1	25	1	27	4
Negative	0	0	1	7	2	16	1	12

Note: The data were presented as number.

Abbreviations: LAD, left anterior descending.

symptomatic hypoglycemia, and two patients experienced asymptomatic hypoglycemia. These conditions were immediately resolved by orally administering 10 g of glucose without impacting image quality. Twelve patients experienced minor symptoms, such as hunger, sweating, dizziness, and elevated heart rate, but with normal BG. They were closely monitored, and their symptoms were resolved after rest. Furthermore, none of the patients experienced discomfort in the FAST group.

Qualitative and Quantitative Imaging Results

Fig. 2 depicts the distribution of patients with different scores in the G/I and FAST groups. Although the imaging score of G/I group (4.36 ± 0.94) was higher than that of FAST group (3.55 ± 1.09, $p < 0.001$), there were no non-diagnostic images in the FAST group. The G/I and FAST imaging scores were identical for 18 patients in both groups. A representative case of equivalent qualitative and quantitative results obtained using both G/I and FAST methods is shown in Fig. 3. Moreover, in one patient, the FAST-imaging score (score 4) was higher than the G/I-imaging score (score 3).

In the G/I group, only one patient was found without hibernating myocardium, whereas in the FAST group, hibernating myocardium was observed in all patients (Fig. 4). The distribution of positive or negative findings in the LAD, LCX, and RCA between the G/I and FAST groups is shown in Table 3. G/I and FAST methods indicated strong agreement for positive and negative outcomes in LAD, LCX, and RCA (κ = 0.847, 0.858, and 0.74, respectively). The discrepancies in positive and negative findings for LCX and RCA between the G/I and FAST methods are depicted in Fig. 5.

Journal of
BIOLOGICAL REGULATORS
and Homeostatic Agents

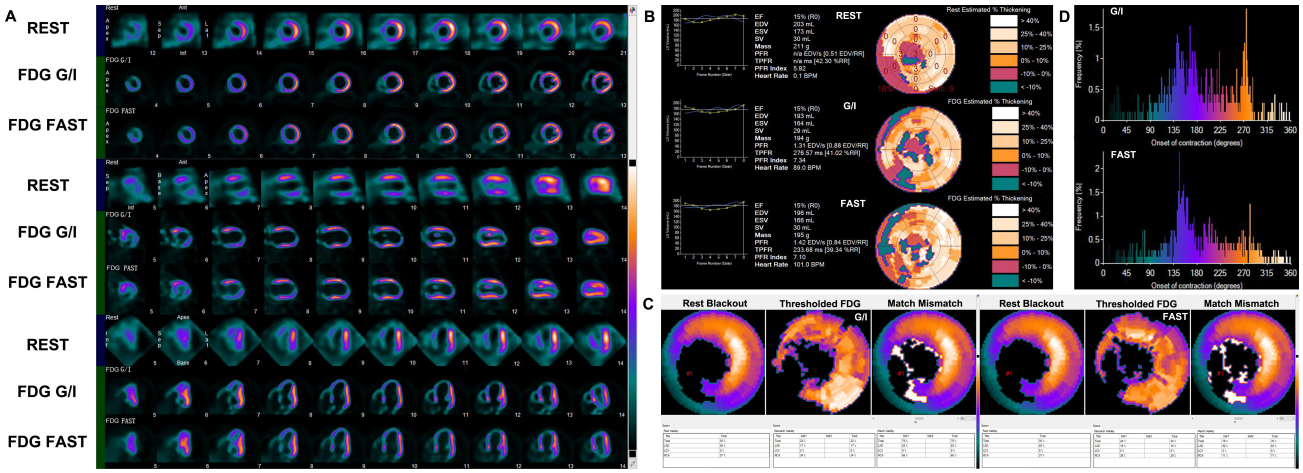

Fig. 3. Equivalent qualitative and quantitative results in positron emission tomography (PET) imaging for evaluating myocardial viability using the G/I and FAST protocol in a 65-year-old male with ischemic cardiomyopathy. (A) Short axis, vertical long-axis, and horizontal long-axis of perfusion-metabolic images (both PET images score 5). (B) Left ventricular ejection fraction (LVEF) and left ventricle (LV) wall thickening estimation. (C) Myocardial viability assessment on polar map. (D) Poor LV dyssynchrony using the G/I and FAST protocols.

Table 4. Qualitative and quantitative imaging results.

	G/I	FAST	*p*-value	*t*/*Z* value
5-point score	4.36 ± 0.94	3.55 ± 1.09	<0.001*	5.216
SUVmeanBlood	0.76 ± 0.30	1.14 ± 0.22	<0.001*	–10.372
SUVmaxMyo	11.70 (7.80–14.78)	8.46 (4.59–14.34)	0.007*	–2.696[b]
M/B	15.16 (9.23–25.84)	6.98 (4.03–13.29)	<0.001*	–4.983[b]
Polar map-mismatch (50% threshold)				
Total (%)	46.00 (25.00–81.25)	64.00 (34.75–88.00)	0.015*	–2.422[b]
LAD (%)	40.50 (10.50–77.25)	68.50 (16.25–91.00)	0.034*	–2.118[b]
LCX (%)	20.00 (0.00–89.50)	23.50 (0.00–89.75)	0.966	–0.043[b]
RCA (%)	20.50 (0.00–69.25)	45.00 (0.00–93.75)	0.011*	–2.530[b]
Polar map-mismatch (50% threshold) (score 3–5 in FAST, n = 33)				
Total (%)	51.00 (25.50–80.50)	58.00 (29.50–81.00)	0.321	–0.992[b]
LAD (%)	47.00 (18.00–82.50)	62.00 (17.50–87.50)	0.333	–0.969[b]
LCX (%)	16.00 (0.00–80.50)	22.00 (0.00–75.00)	0.506	–0.665[c]
RCA (%)	22.00 (0.00–68.50)	40.00 (0.00–74.00)	0.271	–1.102[b]
Dyssynchrony				
Peak phase	132.55 ± 49.47	145.32 ± 57.32	0.132	–1.534
Standard deviation	77.41 ± 16.19	76.87 ± 16.93	0.848	0.193
Histogram bandwidth	257.23 ± 41.58	252.57 ± 51.59	0.559	0.589
Histogram skewness	1.84 ± 0.67	1.86 ± 0.64	0.856	–0.182
Histogram kurtosis	3.30 (1.95–5.30)	3.50 (2.30–6.18)	0.294	–1.050[b]
PET LVEF (%)	24.98 ± 11.54	25.16 ± 10.78	0.737	–0.338

Note: Normally distributed data were presented as mean ± SD and non-normally distributed data were presented as the median and the interquartile range.

*p-value < 0.05 in comparison between G/I and FAST groups; [b], based on negative ranks; [c], based on positive ranks.

Abbreviations: n, number of patients; SUVmeanBlood, SUVmean of blood pool; SUVmaxMyo, SUVmax of the whole left ventricular muscle; M/B, SUVmeanBlood and SUVmaxMyo ratio.

There were substantial differences in SUVmeanBlood, SUVMyo, and M/B between the G/I and FAST groups ($p < 0.001$, $p = 0\ 007$, $p < 0.001$, respectively). The extent of perfusion-metabolism mismatch with the 50% threshold on the polar map was compared for the whole self-controlled cohort (n = 44) and those with scores ranging from 3–5 (with FAST protocol, n = 33). These findings are summarized in Table 4. For patients with scores ranging

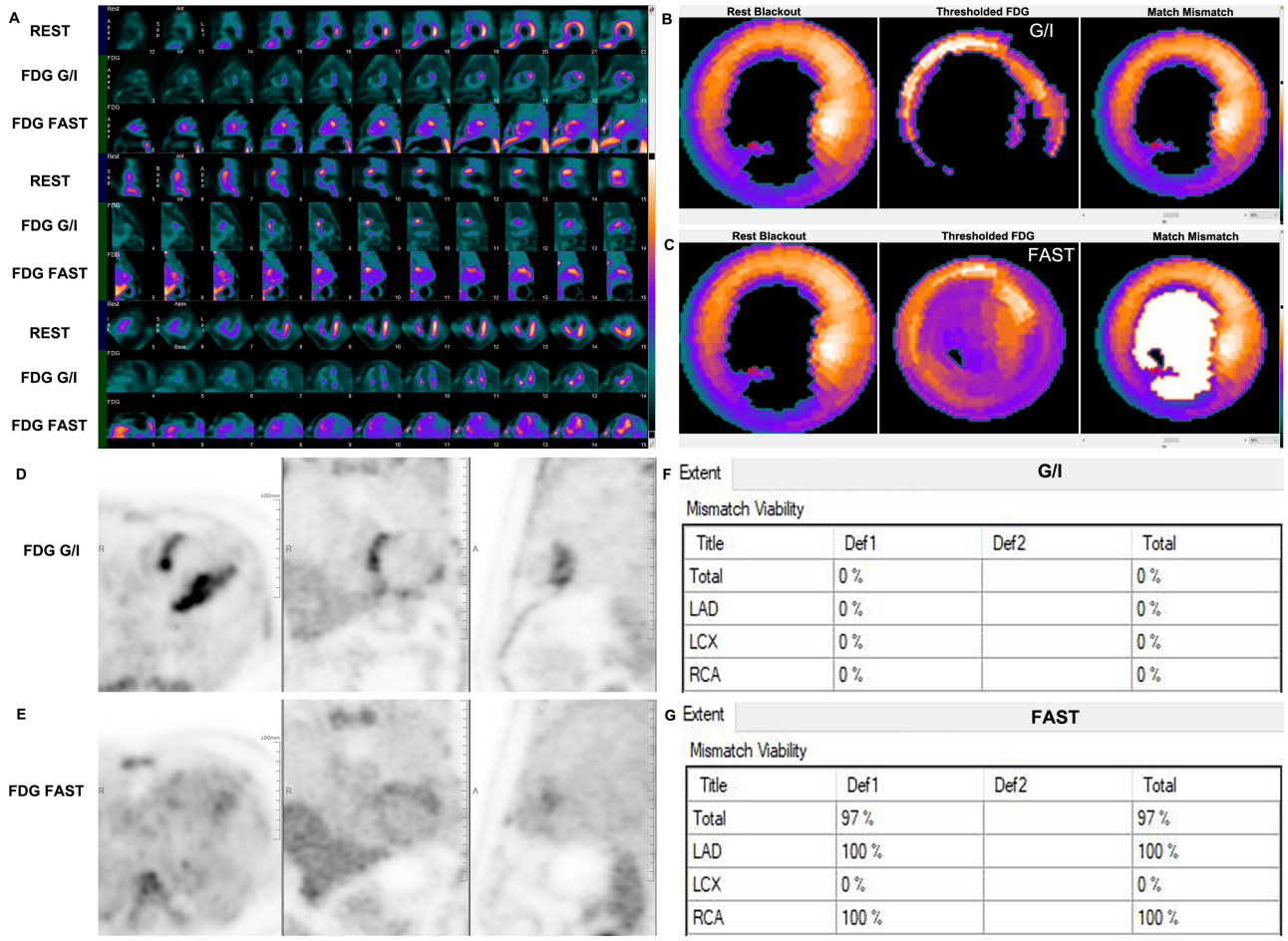

Fig. 4. Fluorodeoxyglucose (FDG) PET imaging using the G/I and FAST methods yielded the opposite assessment of hibernating myocardium. (A) Rest myocardial perfusion imaging (MPI) with short, vertical, and horizontal long-axis images demonstrated a severe perfusion defect in the apical, anterior walls, septal walls, and inferior walls, indicating minimal to no FDG uptake under the G/I method but slight to mild FDG avidity with the FAST protocol. This was evident on the polar map ((B) for G/I and (C) for FAST). The total mismatch viability extent was 0% and 97% in the G/I (F) and FAST (G) groups, respectively. The FDG imaging score was 5 for G/I and 2 for FAST. Furthermore, higher FDG uptake was observed in the LV blood pool with FAST (E) compared to G/I (D), with SUVmean of blood pool (SUVmeanBlood) values of 1.52 and 0.78, respectively.

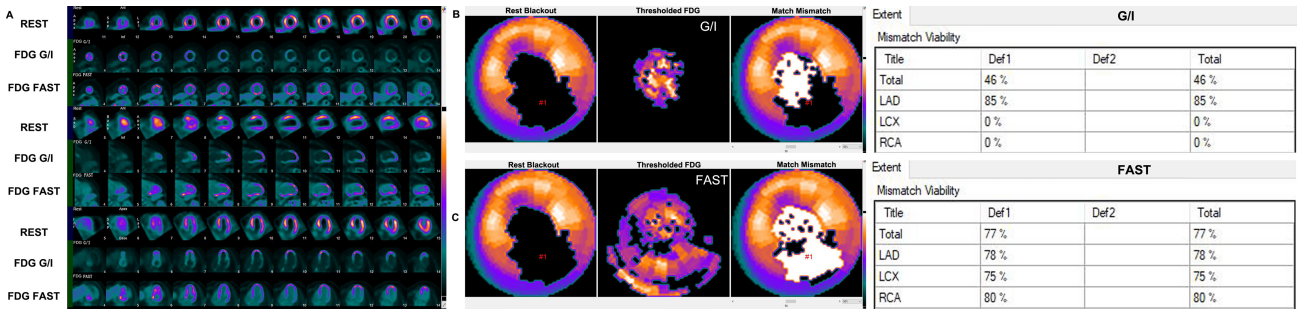

Fig. 5. Metabolic imaging conducted on a 61-year-old woman with ischemic cardiomyopathy revealed hibernating myocardium in left circumflex (LCX) (75%) and right coronary artery (RCA) (80%) in the FAST group, whereas they were negative in the G/I group. (A) Three-dimensional heart image slices from rest MPI, FDG PET with G/I (score 4) and with FAST (score 3). (B,C) Myocardial viability assessment on polar maps and mismatch viability extent results using the G/I and FAST.

from 3 to 5 (with FAST protocol), myocardial viability assessment exhibited equivalence between the groups (all $p > 0.05$). Assessment of LV Dyssynchrony and LVEF exhibited no significant differences between the groups (all

Journal of
BIOLOGICAL REGULATORS
and Homeostatic Agents

Table 5. Relationship between the image score and significant parameters and predictors for qualitative estimation (5-point score).

	5-point score							
	G/I				FAST			
Spearman correlations	*p*-value	95% confidence interval			*p*-value	95% confidence interval		
FBG	0.0674	–0.54∼0.03			0.0066†	–0.63∼–0.11		
Pre-inject BG	0.0160*	–0.60∼–0.06			0.0066†	–0.63∼–0.11		
Pre-image BG	0.0134*	–0.61∼–0.07			0.0607	–0.54∼0.02		
PBG	0.0662	–0.03∼0.54						
Insulin	0.0055*	0.13∼0.65						
SUVmeanBlood	0.0001*	–0.73∼–0.29			0.0965	–0.52∼0.06		
SUVmaxMyo	<0.0001*	0.57∼0.86			<0.0001†	0.79∼0.94		
M/B	<0.0001*	0.65∼0.89			<0.0001†	0.77∼0.93		
Multivariable linear regression	*p*-value	95% confidence interval	B	S.E.	*p*-value	95% confidence interval	B	S.E.
Pre-inject BG	0.5519	–0.47∼0.25	–0.107	0.178	0.8798	–0.13∼0.12	–0.009	0.062
Pre-image BG	0.7452	–0.36∼0.26	–0.049	0.151				
Insulin	0.0140**	0.03∼0.27	0.152	0.059				
SUVmeanBlood	0.0793	–2.91∼0.17	–1.368	0.757				
SUVmaxMyo	0.0005**	0.07∼0.24	0.154	0.040	0.0003††	0.09∼0.29	0.190	0.047
M/B	0.1439	–0.08∼0.01	–0.033	0.022	0.3128	–0.12∼0.04	–0.040	0.039

*p-value < 0.05 in Spearman correlations between 5-point score and significant parameters (FBG, pre-inject BG, pre-image BG, PBG, insulin, SUVmeanBlood, SUVmaxMyo, and M/B) in the G/I group.

†p-value < 0.05 in Spearman correlations between 5-point score and significant parameters (FBG, pre-inject BG, pre-image BG, SUVmeanBlood, SUVmaxMyo, and M/B) in the FAST group.

**p-value < 0.05 in Multivariable linear regression between 5-point score and significant parameters (pre-inject BG, pre-image BG, insulin, SUVmeanBlood, SUVmaxMyo, and M/B) in the G/I group.

††p-value < 0.05 in Multivariable linear regression between 5-point score and significant parameters (pre-inject BG, SUVmaxMyo, and M/B) in the FAST group.

In the FAST group, FBG was pre-inject BG.

$p > 0.05$). However, both LVEF from metabolic imaging (PET LVEF) under G/I (24.98% ± 11.54%) and FAST (25.16% ± 10.78%) was significantly lower than that from ECD (37.80% ± 9.61%, both $p < 0.01$).

The binary logistic regression analysis model for predicting metabolic imaging score employing G/I (coefficient of determination (R^2) = 0.6226) revealed significant predictors such as insulin consumption (95% confidence interval (CI) 0.03–0.27, $p = 0.014$) and SUVmaxMyo (95% CI 0.07–0.24, $p = 0.0005$). Similarly, the binary logistic regression analysis model for predicting the metabolic imaging score with FAST (coefficient of determination (R^2) = 0.6787) identified SUVmaxMyo (95% CI 0.09–0.29, $p = 0.0003$) as a significant predictor (Table 5).

Discussion

PET imaging for assessing myocardial viability in ischemia involves a combination of rest MPI and metabolic imaging using ^{18}F-FDG. ^{18}F-FDG PET can assist in decision-making for ICM [20]. Myocardial revascularization is recommended to improve myocardial function and prognosis in ICM and is widely practiced [21]. Recently, Xu *et al.* [4] reported the importance of detecting hibernating myocardium using PET to predict improved left heart function after CABG. There are various protocols for ^{18}F-FDG metabolic imaging, with glucose loading being the most widely used. Our study aimed to evaluate FDG metabolic imaging with a protocol known as FAST, compared to the G/I method, to meet the personalized clinical needs for myocardial viability assessment.

The significant findings in this prospective self-controlled study were as follows: (1) The G/I and FAST protocols showed strong agreement (all $\kappa > 0.7$) in identifying positive and negative findings in the LAD, LCX, and RCA, indicating their efficacy in evaluating hibernating myocardium assessment. (2) No patients were observed demonstrating non-diagnostic image quality. (3) Quantitative assessment of myocardial viability using the FAST technique, particularly with imaging scores ranging from 3–5 (75%), was comparable to that obtained with the G/I method. (4) Importantly, patients did not report discomfort during the procedure with the FAST protocol. All these findings indicate that the FAST protocol is both time-efficient and safer, providing potential significance for the clinical utility of ^{18}F-FDG PET in myocardial viability assessment, especially in conditions involving a high risk of

hypoglycemia or poor tolerance. Interestingly, in one patient, hibernating myocardium was observed with FAST but not with the G/I method, resulting in a substantial change in clinical treatment decisions, with the patient subsequently undergoing CABG.

However, it is important to recognize that in our study, 25% of patients exhibited fair image quality, which may have contributed to the overestimation of viable myocardium, consistent with previous reports [22]. This is because as the blood inside LV increases, the number of counts increases accordingly due to limitations of reconstruction algorithms [23]. Because the semiquantitative images are always normalized to the pixel with the highest activity and presented visually on a linear scale, images of suboptimal quality overestimate viability and underestimate scar [24].

Moreover, we identified significant predictors for the qualitative quality of metabolic imaging using the G/I technique (insulin consumption and SUVmaxMyo) and the FAST protocol (SUVmaxMyo). These observations align with the effect of insulin on myocardial function and its impact on achieving optimal glucose loading. Insulin is the most robust stimulant for GLUT4 redistribution to the plasma membrane [22,23], directly stimulating myocardial uptake of ^{18}F-FDG. Chen *et al*. [24] proposed an intravenous regular insulin protocol, which led to a higher ratio of interpretable cardiac PET images (100%) compared to the standard glucose loading group (83.3%, $p = 0.026$). More attention should be paid to diabetic patients in case of hypoglycemia since larger amount insulin would be used to maintain image quality. In our study, all cardiac PET images were interpretable in the FAST group without any instances of hypoglycemia.

We also compared the LV dyssynchrony between the G/I and FAST groups. We did not observe any significant differences between these two conditions. Some studies have demonstrated that assessing LV mechanical dyssynchrony (LVMD) through phase analysis may provide additional prognostic value in patients with heart disease [25,26], particularly utilizing SPECT imaging, while few studies have investigated this with FDG PET. Tian *et al*. [27] compared the LV phase dyssynchrony parameters obtained from ^{99m}Tc-MIBI SPECT (GSPECT) and ^{18}F-FDG PET (GPET) and evaluated the prognostic values in ICM patients. They suggested that the phase parameters achieved from GSPECT and GPET were not interchangeable in ICM patients, and patients with LV dyssynchrony measured by gated SPECT exhibited a worse outcome.

In contrast, Pazhenkottil *et al*. [28] reported an excellent agreement between GPET and GSPECT in assessing LVMD among 30 CAD subjects. They demonstrated correlation coefficients of 0.88 for both bandwidth and standard deviation. Shao *et al*. [29] explored phase analysis of gated myocardial metabolic imaging to objectively assess LV systolic dyssynchrony resulting from interactions among multiple factors in Bama mini-pigs after myocardial infarction. As a reflection of myocardium viability, LV dyssynchrony derived from FDG PET may be relevant, but further validation is needed in future investigations.

In our study, patients underwent ^{18}F-FDG PET imaging 2 hours after FDG injection. We adopted this interval to minimize the impact of delayed clearance of pooled activity or insufficient time for tracer clearance.

This study had several limitations. Firstly, due to its pilot nature, the study population was small and limited to ICM patients undergoing evaluation. We are now trying our best to collect more clinical samples, and future studies will verify our current conclusions with additional clinical samples. Secondly, it was a single-center study, underscoring the need for data from multiple centers to conduct multi-center investigations that can improve the generalizability of the present study's findings. Thirdly, we did not use additional measures to manage the suboptimal imaging quality. Lastly, this study lacked long-term follow-up data, which will be addressed in our future research to assess the longevity of treatment effects and the long-term prognosis of the patients. Future research with larger, multi-center, and more different protocol cohorts is warranted for a comprehensive assessment of the outlined parameters. The present study compared two methods in patients with ischemic cardiomyopathy, focusing on image quality, viability scope, and left ventricular asynchrony to explore their suitability for clinical practice. The study provides two viable methods for assessing myocardial viability in ischemic cardiomyopathy. It compares the advantages and limitations of these methods in practical applications, aiding clinicians in choosing the appropriate assessment protocol based on patient conditions. Additionally, it provides a scientific basis for decision-making, especially in assessing myocardial feasibility before coronary artery reconstruction surgery, which is crucial for improving surgical success rates and patient prognosis.

Conclusions

In summary, our findings suggest that the FAST protocol is time-efficient and safe for the clinical utility of ^{18}F-FDG PET in myocardial viability assessment compared to the G/I protocol.

Availability of Data and Materials

The dataset used and/or analyzed in the current study are available from the corresponding authors on reasonable request.

Author Contributions

HS and TG contributed to the study conception and design. Material preparation, data collection, image review and interpretation, data analysis were performed by TG and WM. HY and SC assisted in image acquisition and process-

Journal of
BIOLOGICAL REGULATORS
and Homeostatic Agents

ing. XW performed experiments and cared patients. The draft of the manuscript was written by TG. HS, TG and WM contributed to the manuscript's revision. All authors have been involved in revising it critically for important intellectual content. All authors gave final approval of the version to be published. All authors have participated sufficiently in the work to take public responsibility for appropriate portions of the content and agreed to be accountable for all aspects of the work in ensuring that questions related to its accuracy or integrity.

Ethics Approval and Consent to Participate

Written informed consent was obtained from all individual participants (patients) in this study. This study was performed in line with the principles of the Declaration of Helsinki. This study was approved by the Medical Ethics Committee of Zhongshan Hospital, Fudan University (B2022-280R).

Acknowledgment

The authors want to thank the PET/CT technologists from the Zhongshan Hospital, Fudan University for assistance with the PET/CT scans.

Funding

This research received no external funding.

Conflict of Interest

The authors declare no conflict of interest.

References

[1] Neumann FJ, Sousa-Uva M. 'Ten commandments' for the 2018 ESC/EACTS Guidelines on Myocardial Revascularization. European Heart Journal. 2019; 40: 79–80.

[2] Dilsizian V, Bacharach SL, Beanlands RS, Bergmann SR, Delbeke D, Dorbala S, *et al*. ASNC imaging guidelines/SNMMI procedure standard for positron emission tomography (PET) nuclear cardiology procedures. Journal of Nuclear Cardiology. 2016; 23: 1187–1226.

[3] Sarikaya I, Elgazzar AH, Alfeeli MA, Sharma PN, Sarikaya A. Status of F-18 fluorodeoxyglucose uptake in normal and hibernating myocardium after glucose and insulin loading. Journal of the Saudi Heart Association. 2018; 30: 75–85.

[4] Xu D, Zhang J, Liu B, Fu D, Li J, Fan L. Determination of viable myocardium through delayed enhancement cardiac magnetic resonance imaging combined with ^{18}F-FDG PET myocardial perfusion/metabolic imaging before CABG. The International Journal of Cardiovascular Imaging. 2024; 40: 887–895.

[5] Sarikaya I, Sharma PN, Sarikaya A, Elgazzar AH. Assessing oral glucose and intravenous insulin loading protocol in ^{18}F-fluorodeoxyglucose positron emission tomography cardiac viability studies. World Journal of Nuclear Medicine. 2020; 19: 1–7.

[6] Knuuti MJ, Nuutila P, Ruotsalainen U, Saraste M, Härkönen R, Ahonen A, *et al*. Euglycemic hyperinsulinemic clamp and oral glucose load in stimulating myocardial glucose utilization during positron emission tomography. Journal of Nuclear Medicine. 1992; 33: 1255–1262.

[7] Vitale GD, deKemp RA, Ruddy TD, Williams K, Beanlands RS. Myocardial glucose utilization and optimization of (18)F-FDG PET imaging in patients with non-insulin-dependent diabetes mellitus, coronary artery disease, and left ventricular dysfunction. Journal of Nuclear Medicine. 2001; 42: 1730–1736.

[8] Mhlanga J, Derenoncourt P, Haq A, Bhandiwad A, Laforest R, Siegel BA, *et al*. ^{18}F-FDG PET in Myocardial Viability Assessment: A Practical and Time-Efficient Protocol. Journal of Nuclear Medicine. 2022; 63: 602–608.

[9] Chen YC, Pan MJ, Wang QQ, Wang YH, Zhuo HL, Dai RZ. Intravenous insulin injection supplemented with subsequent milk consumption is a safer formulation for cardiac viability ^{18}F-FDG imaging. Journal of Nuclear Cardiology. 2022; 29: 1985–1991.

[10] Sun XX, Li S, Wang Y, Li W, Wei H, He ZX. Rescue Protocol to Improve the Image Quality of 18F-FDG PET/CT Myocardial Metabolic Imaging. Clinical Nuclear Medicine. 2021; 46: 369–374.

[11] Shao X, Chen Y, Chen Y, Zhang F, Zhou M, Niu R, *et al*. Feasibility and application of trimetazidine in ^{18}F-FDG PET myocardial metabolic imaging of diabetic mellitus patients with severe coronary artery disease: A prospective, self-controlled study. Journal of Nuclear Cardiology. 2022; 29: 2497–2507.

[12] Huang G, Lucignani G, Landoni C, Galli L, Paganelli G, Rossetti C, *et al*. Relation between myocardial 18F-FDG uptake in the fasting state and coronary angiography in patients with coronary artery disease. Nuclear Medicine Communications. 1994; 15: 311–316.

[13] Makaryus AN, McFarlane SI. Diabetes insipidus: diagnosis and treatment of a complex disease. Cleveland Clinic Journal of Medicine. 2006; 73: 65–71.

[14] Refardt J. Diagnosis and differential diagnosis of diabetes insipidus: Update. Best Practice & Research. Clinical Endocrinology & Metabolism. 2020; 34: 101398.

[15] Christ-Crain M, Winzeler B, Refardt J. Diagnosis and management of diabetes insipidus for the internist: an update. Journal of Internal Medicine. 2021; 290: 73–87.

[16] Maes AF, Borgers M, Flameng W, Nuyts JL, van de Werf F, Ausma JJ, *et al*. Assessment of myocardial viability in chronic coronary artery disease using technetium-99m sestamibi SPECT. Correlation with histologic and positron emission tomographic studies and functional follow-up. Journal of the American College of Cardiology. 1997; 29: 62–68.

[17] Skali H, Schulman AR, Dorbala S. 18F-FDG PET/CT for the assessment of myocardial sarcoidosis. Current Cardiology Reports. 2013; 15: 1–11.

[18] Kobylecka M, Mazurek T, Fronczewska-Wieniawska K, Fojt A, Słowikowska A, Mączewska J, *et al*. Assessment of the myocardial FDG-PET image quality with the use of maximal Standardized Uptake Value myocardial to background index. Application of the results in regard to semiquantitative assessment of myocardial viability with cardiac dedicated softwar. Nuclear Medicine Review. Central & Eastern Europe. 2017; 20: 69–75.

[19] Habibzadeh F. Data Distribution: Normal or Abnormal? Journal of Korean Medical Science 2024; 39: e35.

[20] Besenyi Z, Goston G, Hemelein R, Annamária Bakos, László Pávics. Detection of myocardial inflammation by 18f-fdg-pet/ct in patients with systemic sclerosis without cardiac symptoms: a pilot study. Clinical and Experimental Rheumatology. 2019; 119: 88–96.

[21] Liga R, Colli A, Taggart DP, Boden WE, De Caterina R. Myocardial Revascularization in Patients With Ischemic Cardiomyopathy: For Whom and How. Journal of the American Heart Association. 2023; 12: e026943.

[22] Bax JJ, Visser FC, Poldermans D, van Lingen A, Elhendy A, Boersma E, *et al*. Feasibility, safety and image quality of cardiac FDG studies during hyperinsulinaemic-euglycaemic clamping. European Journal of Nuclear Medicine and Molecular Imaging. 2002; 29: 452–457.

[23] Jaldin-Fincati JR, Pavarotti M, Frendo-Cumbo S, Bilan PJ, Klip A. Update on GLUT4 Vesicle Traffic: A Cornerstone of Insulin Action. Trends in Endocrinology and Metabolism. 2017; 28: 597–611.

[24] Ćorović A, Nus M, Mallat Z, Rudd JHF, Tarkin JM. PET Imaging of Post-infarct Myocardial Inflammation. Current Cardiology Reports. 2021; 23: 99.

[25] Coleman RE. Single photon emission computed tomography and positron emission tomography in cancer imaging. Cancer. 1991; 67: 1261.

[26] Cerqueira MD, Harp GD, Ritchie JL. Evaluation of myocardial perfusion and function by single photon emission computed tomography. Seminars in Nuclear Medicine. 1987; 17: 200–213.

[27] Tian Y, Zhao M, Li W, Zhu Z, Mi H, Li X, *et al*. Left ventricular mechanical dyssynchrony analzyed by Tc-99m sestamibi SPECT and F-18 FDG PET in patients with ischemic cardiomyopathy and the prognostic value. The International Journal of Cardiovascular Imaging. 2020; 36: 2063–2071.

[28] Pardini M, Huey ED, Spina S, Kreisl WC, Grafman J. FDG-PET patterns associated with underlying pathology in corticobasal syndrome. Neurology. 2019; 92: e1121–e1135.

[29] Shao X, Wang J, Tian Y, Fan S, Zhang F, Yang W, *et al*. Role of Gated Myocardial Glucose Metabolic Imaging in Assessing Left Ventricular Systolic Dyssynchrony after Myocardial Infarction and the Influential Factors. Scientific Reports. 2018; 8: 11178.